RESEARCH ARTICLE

Proteome analysis identifies novel protein candidates involved in regeneration of the cerebellum of teleost fish

*Marianne M. Zupanc, Ursula M. Wellbrock and Günther K. H. Zupanc**

School of Engineering and Science, International University Bremen, Bremen, Germany

Received: March 18, 2005
Accepted: June 14, 2005

In contrast to mammals, adult teleost fish exhibit an enormous potential to regenerate neuronal tissue after injuries to the CNS. By combining a well-defined cerebellar lesion paradigm with differential proteome analysis at a post-lesion survival time of 3 days, we screened for protein candidates involved in repair of the fish brain. Out of nearly 900 protein spots detected on 2-D gels, spot intensity was significantly increased at least twofold in 30 spots and decreased to at least half the intensity of control tissue in 23 spots. The proteins associated with 24 of the spots were identified by PMF and MS/MS fragmentation. The cellular localization and the spatio-temporal patterns of two of these proteins, beta-actin and beta-tubulin, were further characterized through immunohistochemistry. Comparison of the observed changes in protein abundance with the previously characterized events underlying regeneration of the cerebellum suggests that the proteins identified are especially involved in cellular proliferation and survival, as well as axonal sprouting.

Keywords:
Adult neurogenesis / *Apteronotus leptorhynchus* / Axonal regeneration / Neuronal regeneration / Wound healing

1 Introduction

Unlike mammals, neural tissue in adult teleost fish heals quickly and efficiently after injuries applied to the CNS. The regenerative capability includes not only regrowth of axons (axonal regeneration) but also the replacement of whole neurons by newly generated ones (neuronal regeneration) (for reviews, see [1–4]). This difference between fish and mammals makes it particularly attractive to study regeneration in the former taxon, as identification of the cellular mechanisms mediating regeneration in fish is likely to provide important insights into the factors limiting this phenomenon in mammals.

Correspondence: Prof. Dr. Günther K. H. Zupanc, International University Bremen, School of Engineering and Science, P.O. Box 750 561, 28725 Bremen, Germany
E-mail: g.zupanc@iu-bremen.de
Fax: +49-421-200-493244

Abbreviations: BMZF2, bone marrow zinc finger 2; **BPAG1**, bullous pemphigoid antigen 1; **CCb**, corpus cerebelli; **GFAP**, glial fibrillary acidic protein; **gra**, granular layer; **K10**, keratin-10; **mol**, molecular layer; **NGF**, nerve growth factor; **RT**, room temperature

In fish, regeneration of brain tissue is accomplished by a series of well-orchestrated processes. One of the first events after application of a mechanical lesion to the teleostean cerebellum is detectable as early as a few minutes after the injury, when damaged cells undergo apoptosis [5]. In mammals, necrotic cell death dominates after brain injuries [6], and only a minor portion of the cells die through apoptotic cell death (for reviews, see [7, 8]).

The occurrence of apoptotic cell death after lesions in the teleostean cerebellum is supplemented by the removal of cellular debris by microglia and macrophages [9]. Their number increases approximately 3 days after the lesion and reaches maximum levels at roughly 10 days.

The clearance of cellular debris is paralleled by the restoration of lost neuronal tissue through recruitment of new neurons. The majority of these cells originate from proliferation zones that supply progenitors of new neurons in the intact brain [10–13]. A minor portion of the new cells is

* Dedicated to Theodore H. Bullock, Professor Emeritus at the University of California, San Diego, on the occasion of his 90th birthday on 16 May 2005.

produced directly around the site of the lesion by mitotic division of stem cells that are quiescent in the intact brain. In either of the two stem cell populations, the production of new cells displays a several-fold increase between 1 and 10 days after the lesion.

The new cells are guided to the lesion site by radial glial fibers characterized by their immunoreactivity against glial fibrillary acidic protein (GFAP). The density of such GFAP-positive fibers increases in the vicinity of the lesion approximately 8 days after the lesion and remains elevated for at least 100 days [14]. The persistence of GFAP-positive fibers, as well as a similar continued presence of vimentin-immunolabeled fibers [15], suggests that these intermediate filament proteins may also be involved in later developmental processes, such as survival or differentiation of the new cells.

Although the spatiotemporal patterns of the major processes underlying regeneration of neural tissue in the adult fish brain are fairly well characterized, little is known about the molecular factors mediating them. Therefore, in the present investigation, we combined differential proteome analysis with a well-defined lesion paradigm in a standard teleostean model system, the brown ghost knifefish (*Apteronotus leptorhynchus*). In using this approach, we have succeeded in the large-scale identification of novel protein candidates involved in the repair of the teleostean brain.

2 Materials and methods

2.1 Animals

Brown ghost knifefish (*Apteronotus leptorhynchus*; Gymnotiformes, Teleostei) were supplied by a tropical fish importer (Aquarium Glaser, Rodgau, Germany). The fish were kept in 45-L and 300-L tanks at temperatures of approximately 27°C and exposed to a 12-h light/12-h dark photoperiod. The conductivity of the water was kept at about 150–250 μS/cm, and the pH was roughly 7. The fish were fed frozen mosquito larvae daily.

A total of 37 fish were used in this study. Their morphological characteristics are listed in Table 1. Post-mortem gonadal inspection demonstrated that 18 of these fish were male, and 19 were female. Total length ranged between 102 mm and 149 mm (mean: 118 mm; median: 115 mm; SD: 10 mm) and body weight between 2.1 g and 5.4 g (mean: 3.3 g; median: 3.3 g; SD: 0.7 g), suggesting that all the individuals can be regarded as adults. The gonadosomatic index (gonad weight divided by body weight) of the fish ranged between 0.0004 and 0.0043 in males (mean: 0.0017; median: 0.0015; SD: 0.0009) and 0.0052 and 0.0725 in females (mean: 0.0159; median: 0.0102; SD: 0.0150). This suggests that most of the individuals of this seasonally breeding species were not reproductively active at the time of inspection.

2.2 Application of cerebellar lesions

Mechanical lesions were applied to the dorsal-most subdivision of the cerebellum, the corpus cerebelli (CCb), as described previously [5, 9, 13–15]. Individual fish were subjected to general anesthesia by immersion into aquarium water containing approximately 2% ethyl carbamate ("urethane"; Sigma-Aldrich, Munich, Germany) and locally anesthetized on the head with 2% lidocaine solution (Caesar & Loretz, Hilden, Germany). Guided by landmarks on the fish's head, a 3-mm-deep stab wound was created with a sterile scalpel (no. 11, Feather) such that an approximately 1-mm-deep cut traveling in parasagittal direction within the CCb was produced (Fig. 1). After recovery in oxygenated aquarium water, the fish were transferred to isolation tanks for various post-lesion survival times, as indicated in Table 1. All experiments were carried out in accordance with the regulations of the relevant German law, the *Deutsches Tierschutzgesetz* of 1998.

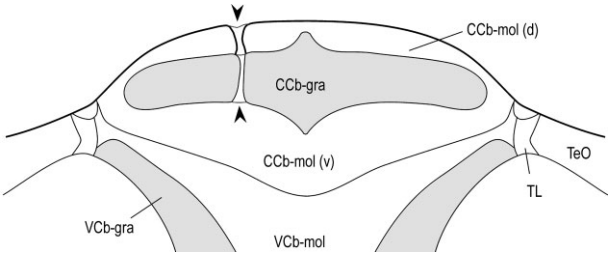

Figure 1. Schematic representation of the lesioning paradigm. The stab-wound lesion (arrowheads) was applied unilaterally to the corpus cerebelli such that the scalpel penetrated both the dorsal molecular layer (CCb-mol(d)) and the granular layer (CCb-gra) and that the path of lesion was located roughly halfway between the midline of the brain and the lateral edge of the granule cell layer. CCb-mol(v), ventral molecular layer of corpus cerebelli; TeO, optic tectum; TL, torus longitudinalis; VCb-gra, granule cell layer of valvula cerebelli; VCb-mol, molecular layer of valvula cerebelli.

The location and extent of the lesion were consistent among individual fish. The path of the lesion ran parallel to the midline of the brain through the dorsal molecular layer (mol) of the CCb and the adjacent granular layer (gra). The lesion was positioned roughly halfway between the midline and the lateral edge of CCb-gra.

2.3 Isolation of brain tissue for proteome analysis

For proteome analysis, a total of ten fish were used. In five of these fish, the CCb was lesioned as described in Section 2.2. Three days after setting the lesion, these fish were killed by immersion into an overdose of 3-aminobenzoic acid ethyl ester (Sigma-Aldrich) dissolved in aquarium water. Their heads were cooled with pieces of crushed ice and the skulls were opened. A block was dissected out of the CCb such that an approximately 0.5-mm-thick rim of tissue surrounded the path of lesion. This piece of tissue was immediately frozen in

Table 1. Morphological characteristics of the fish used in the experiments

Fish	Total length (mm)	Body weight (g)	Sex[a)]	Relative gonadal weight[b)]	Treatment	Post-lesion survival time	Experiment[c)]
MZ-IUB-1	112	2.67	Female	0.0177	Lesion	3 days	Proteomics
MZ-IUB-3	123	3.39	Female	0.0190	Lesion	3 days	Proteomics
MZ-IUB-4	108	2.79	Male	0.0004	Lesion	3 days	Proteomics
MZ-IUB-5	110	2.73	Male	0.0011	Lesion	3 days	Proteomics
MZ-IUB-6	110	2.87	Male	0.0043	Lesion	3 days	Proteomics
MZ-IUB-7	106	2.07	Male	0.0010	Intact	n/a	Proteomics
MZ-IUB-8	119	2.62	Female	0.0177	Intact	n/a	Proteomics
MZ-IUB-9	115	3.47	Female	0.0154	Intact	n/a	Proteomics
MZ-IUB-10	102	2.23	Male	0.0014	Intact	n/a	Proteomics
MZ-IUB-11	128	3.74	Male	0.0016	Intact	n/a	Proteomics
UW-IUB-35	115	2.75	Female	0.0101	Intact	n/a	IHC: β-actin
UW-IUB-38	110	3.04	Male	0.0007	Intact	n/a	IHC: β-actin
UW-IUB-44	116	3.25	Male	0.0020	Intact	n/a	IHC: β-actin, β-tubulin
UW-IUB-45	130	5.36	Male	0.0022	Intact	n/a	IHC: β-actin, β-tubulin
GZ-IUB-78	115	2.72	Female	0.0080	Lesion	6 h	IHC: β-actin, β-tubulin
GZ-IUB-79	132	3.84	Female	0.0725	Lesion	6 h	IHC: β-actin, β-tubulin
GZ-IUB-60	115	2.66	Male	0.0032	Lesion	1 day	IHC: β-actin, β-tubulin
GZ-IUB-61	124	3.27	Female	0.0152	Lesion	1 day	IHC: β-actin, β-tubulin
GZ-IUB-66	112	3.33	Female	0.0085	Lesion	2 days	IHC: β-actin, β-tubulin
GZ-IUB-67	113	3.31	Female	0.0052	Lesion	2 days	IHC: βactin, β-tubulin
GZ-IUB-55	117	3.57	Female	0.0066	Lesion	3 days	IHC: β-actin
GZ-IUB-58	149	4.69	Female	0.0156	Lesion	3 days	IHC: β-actin
GZ-IUB-59	128	4.47	Male	0.0015	Lesion	3 days	IHC: β-actin
GZ-IUB-80	115	2.60	Male	0.0015	Lesion	4 days	IHC: control β-actin
GZ-IUB-88	108	2.85	Female	0.0096	Lesion	4 days	IHC: control β-tubulin
GZ-IUB-72	120	3.37	Male	0.0012	Lesion	5 days	IHC: β-actin, β-tubulin
GZ-IUB-73	105	3.73	Female	0.0066	Lesion	5 days	IHC: β-actin, βtubulin
GZ-IUB-68	130	3.56	Female	0.0178	Lesion	10 days	IHC: β-actin, βtubulin
GZ-IUB-74	135	3.28	Male	0.0011	Lesion	10 days	IHC: β-actin, β-tubulin
GZ-IUB-70	114	3.48	Female	0.0102	Lesion	15 days	IHC: β-actin, β-tubulin
GZ-IUB-75	124	3.93	Male	0.0012	Lesion	15 days	IHC: β-actin, β-tubulin
GZ-IUB-76	117	3.43	Female	0.0298	Lesion	30 days	IHC: β-actin, β-tubulin
GZ-IUB-77	136	4.60	Male	0.0016	Lesion	30 days	IHC: β-actin, β-tubulin
GZ-IUB-82	112	2.52	Female	0.0091	Lesion	4 days	WB: β-actin, β-tubulin
GZ-IUB-83	108	2.36	Female	0.0079	Lesion	4 days	WB: β-actin, β-tubulin
GZ-IUB-84	113	3.19	Male	0.0015	Lesion	4 days	WB: β-actin, β-tubulin
GZ-IUB-85	118	3.15	Male	0.0023	Lesion	4 days	WB: β-actin, β-tubulin

a) Sex of the fish was determined by post-mortem gonadal inspection
b) Relative gonadal weight was determined as fresh weight of gonads divided by body weight
c) The fish were used for proteome analysis ("Proteomics"), Western blotting ("WB"), or immunohistochemical staining ("IHC") against β-actin or β-tubulin. In the latter case, one out of two series of alternating brain sections was immunolabeled against the respective antigen

isopentane at −45°C, combined with the tissue blocks of the other lesioned fish, and stored at −80°C until further use. In five unlesioned (control) fish, equivalent pieces of cerebellar tissue were obtained by using the same procedure as in the lesioned fish.

2.4 Sample preparation

The five tissue samples of the lesioned and unlesioned fish, respectively, were pooled and dissolved in a lysis buffer consisting of 7 M urea, 2 M thiourea, 4% w/v CHAPS, and 0.5% pharmalyte pH 3–10 (Amersham Biosciences, Freiburg, Germany). The lysates were centrifuged at 12 000 × *g* for 10 min, and the protein content of the supernatant was measured using the Bradford assay system (Sigma-Aldrich).

2.5 2-DE

Protein extracts were separated by 2-D SDS-PAGE, running the pooled samples from the lesioned and unlesioned fish in quadruplicate and triplicate, respectively. For IEF (first dimension), an 18-cm pH 4–7 IPG strip (Immobiline DryStrip

pH 4–7, Amersham Biosciences) was rehydrated overnight. IEF was conducted for 38 700 Vh, using the Multiphor II system (Amersham Biosciences).

For the second dimension, the IPG was equilibrated by rocking it in a 1% solution of DTT for 10 min, followed by 10 min in a 4% solution of iodoacetamide. Together with proteins (Serva, Heidelberg, Germany) as molecular weight standards, the IPG was embedded onto an SDS-PAGE gel with 0.5% w/v agarose in electrode buffer [16]. Gels were run at 13°C and a maximum of 2000 Vh overnight. The gels were stained with SYPRO Ruby (Molecular Probes, Eugene, Oregon, USA).

2.6 Computerized analysis of protein spots

The SYPRO Ruby-stained gels were scanned with a fluorescent image analyzer, model FLA-3000 (Raytest, Straubenhardt, Germany). The images were analyzed, and averaged gels were generated using ProteomeWeaver software (version 2.2; Definiens, Munich, Germany). Spots were included in the averaged gels if they were found in at least 50% of the gels within either the control or the lesion group. Fold changes were calculated based on the intensity of an individual spot in the averaged lesion gel relative to the intensity of its counterpart in the averaged control gel. Changes were considered only if (1) there was at least a twofold increase (= increase in protein abundance) or a twofold decrease (= decrease in protein abundance); (2) the SD of the mean spot intensity within one group was less than 30%; and (3) the intensity difference was statistically significant ($P < 0.05$, *t*-test).

2.7 Protein identification

Protein identification was accomplished by TopLab (Martinsried, Germany). For PMF, the gels were re-stained with CBB. Protein spots were excised from these gels, de-stained, and subjected to in-gel digestion with modified trypsin (Roche Diagnostics, Basel, Switzerland) overnight at 37°C. The extracted peptides were desalted using a C18 Zip-Tip (Millipore, Schwalbach, Germany). For MALDI-TOF-MS, 0.1 μL of the peptide mixture was spotted onto a MALDI-TOF-MS target (Applied Biosystems, Darmstadt, Germany) mixed with 0.1 μL of the DHBS matrix (2,5-dihydroxybenzoic acid : 2-hydroxy-5-methoxy-benzoic acid, 9:1), and analyzed by MALDI-TOF-MS using a Voyager STR instrument (Applied Biosystems) operated in reflector mode. Database searches were done using the software ProFound (Genomic Solutions, Huntingdon, UK). Protein spots that could not be identified unambiguously by PMF were subjected to an MS/MS fragmentation employing a Proteomics Analyzer 4700 (Applied Biosystems). The fragment ions observed in the MS/MS spectra, along with the peptide masses, were used to search the NCBInr database for protein identification *via* MASCOT query (Matrix Science, London, UK).

2.8 Western blotting

For Western blotting, four fish with lesioned CCb were killed 4 days after application of the stab wound by immersion in a lethal dose of 3-aminobenzoic acid ethyl ester (Sigma-Aldrich) dissolved in aquarium water. The fish were placed on ice, and an approximately 500-μm-wide tissue region around the path of the lesion was immediately removed and homogenized in an ice-cold modified RIPA buffer (50 mM Tris-HCl pH 7.4, 1 mM EDTA, 150 mM NaCl, 1% NP-40, 0.25% Na-deoxycholate, 1 mM PMSF, 1 μg/mL aprotinin, 1 μg/mL leupeptin, 1 μg/mL pepstatin A, 1 mM Na_3VO_4, and 1 mM NaF). The whole cerebellum of one mouse, killed by inhalation of an overdose of CO_2, was processed correspondingly and later used for positive control samples. For negative controls, only lysis buffer was used. The total protein concentrations of the fish and mouse lysates were assessed using the Bradford assay system. Proteins (80 μg of *Apteronotus* CCb lysate and 30 μg of mouse cerebellum lysate) were separated by SDS-PAGE (10% acrylamide), as described by Laemmli [16], and subsequently transferred onto Hybond C extra nitrocellulose sheets (Amersham Biosciences) using a transblot SD semi-dry electrophoretic transfer cell (Bio-Rad, Hercules, CA, USA). The membranes were blocked with 5% non-fat milk powder and immunoreacted with primary antibody (mouse anti-β-actin, clone AC-15, Sigma-Aldrich, dilution 1:2500; or rabbit anti-β-tubulin, Delta Biolabs, Campbell, CA, USA, 0.5 ng/mL) for 1 h at room temperature (RT), followed by incubation with a secondary antibody (goat anti-mouse HRP or goat ant-rabbit HRP, dilution 1:35,000; Jackson ImmunoResearch, West Grove, PA, USA) for 1 h at RT. Bound antibody complexes on the immunoblots were detected with the ECL Western blotting system (Amersham Biosciences).

2.9 Immunohistochemistry

For immunohistochemical analysis, individuals with both intact brains and lesioned CCb were used (Table 1). The fish were killed by immersion into an overdose of 3-aminobenzoic acid ethyl ester in aquarium water and intracardially perfused with a flush solution containing 0.1 M phosphate buffer (PB; pH 7.4), 0.9% NaCl, 5 mg/100 mL heparin sodium salt (research grade, 186 000 IU/g; Serva), and 1 mL/100 mL 2% lidocaine. After all blood had been washed out, the perfusion was continued with 2% paraformaldehyde (AppliChem, Darmstadt, Germany) in 0.1 M PB. The brains were removed from the skull, post-fixed in the same fixative solution for 1–4 h at 4°C, and cryoprotected in 1 M sucrose in PBS overnight at 4°C. After embedding the brains in a 1:1 mixture of AquaMount (Lerner Laboratories, Pittsburgh, PA, USA) and Tissue Tek O.C.T. Compound (Sakura, Finetek), 15-μm-thick transverse sections were cut on a cryostat (model HM 560; Microm, Walldorf, Germany), thaw-mounted onto gelatine/chrome-alum-coated slides, and stored at −20°C until further use.

The cryosections were dried in a desiccator for 90 min at RT and rehydrated in three changes of 0.1 M TBS, pH 7.5, for 10 min each. In order to permeabilize the tissue and block unspecific binding sites, the sections were treated for 1 h at RT with TBS* (3% sheep serum (Sigma-Aldrich), 1% BSA (AppliChem), 1% teleostean gelatine (Sigma-Aldrich), and 0.3% Triton X-100 (AppliChem) in TBS). They were incubated overnight at 4°C with the same anti-β-actin and anti-β-tubulin antibodies, as used for Western blotting. Each of these antibodies was diluted 1:100 in TBS*. Unbound primary antibody was removed by three rinses in TBS for 10 min each. After treatment in TBS** (3% goat serum (Sigma-Aldrich), 1% BSA (AppliChem), 1% teleostean gelatine (Sigma-Aldrich), and 0.3% Triton X-100 (Sigma-Aldrich) in TBS) for 30 min at RT, antigenic sites were visualized by incubating the sections with a 1:1000 dilution in TBS** of secondary antibodies (goat anti-mouse-Cy3 IgG (H+L)) overnight at 4°C or goat anti-rabbit-Cy3 IgG (H+L) for 90 min at RT, respectively (both from Jackson Immuno Research). Following three washes with TBS for 10 min each and three washes with PBS for 3 min each, the sections were counterstained with 2 μg/mL in PBS of the nuclear dye 4',6-diamidino-2-phenylindoledihydrochloride (DAPI; AppliChem) for 3 min at RT. Finally, the sections were washed three times for 3 min each in PBS and once in PB, embedded in PVA, average M_r 30 000–70 000, containing *n*-propyl gallate (for methodological details, see [17]), and coverslipped.

Control experiments to test the specificity of the primary antibodies included the following: (1a) pre-adsorption with 100 μg actin (Sigma-Aldrich) of the anti-β-actin antiserum, diluted 1:100 in 100 μL antibody diluent, and incubated at 4°C for 6.5 h; (1b) pre-adsorption with 100 μg of the synthetic peptide (Delta Biolabs) used as an immunogen for raising the rabbit polyclonal antibody against β-tubulin, diluted 1:100 in 500 μL PBS, and incubated at 4°C for 8 h; this peptide maps near the amino terminus of human β-tubulin; (2) omission of the primary antibodies. These treatments resulted in abolition of labeling (not shown).

2.10 Microscopic analysis

The sections were examined under a Zeiss Axioskop microscope (Carl Zeiss, Göttingen, Germany). Microphotographs were taken using an AxioCam MRc5 digital photocamera (Carl Zeiss) and AxioVision software (release 4.2) on a computer. For confocal microscopy, specimens were examined on a Zeiss LSM 510 META laser scanning microscope equipped with a Zeiss Axiovert 200 M compound microscope and 20, 40, 63, and 100 × Zeiss objectives. Optical sections were taken at a resolution of 1024 × 1024 pixels using LSM 5 software (version 3.2; Carl Zeiss). Images were processed to improve contrast and brightness using the software programs Adobe Photoshop 6.0 (Adobe Systems, San Jose, CA, USA) and Corel Draw 10 (Corel, Ottawa, Ontario, Canada).

3 Results

3.1 Proteome analysis

3.1.1 Differences in protein expression profiles between intact and lesioned brains

SYPRO-Ruby-stained 2-D maps of proteins in the CCb of intact and lesioned fish were obtained in a reproducible manner. On average, 881 spots per sample in the intact CCb, and 862 spots per sample in the lesioned CCb, were identified (Fig. 2). The range of averaged differential spot intensities in

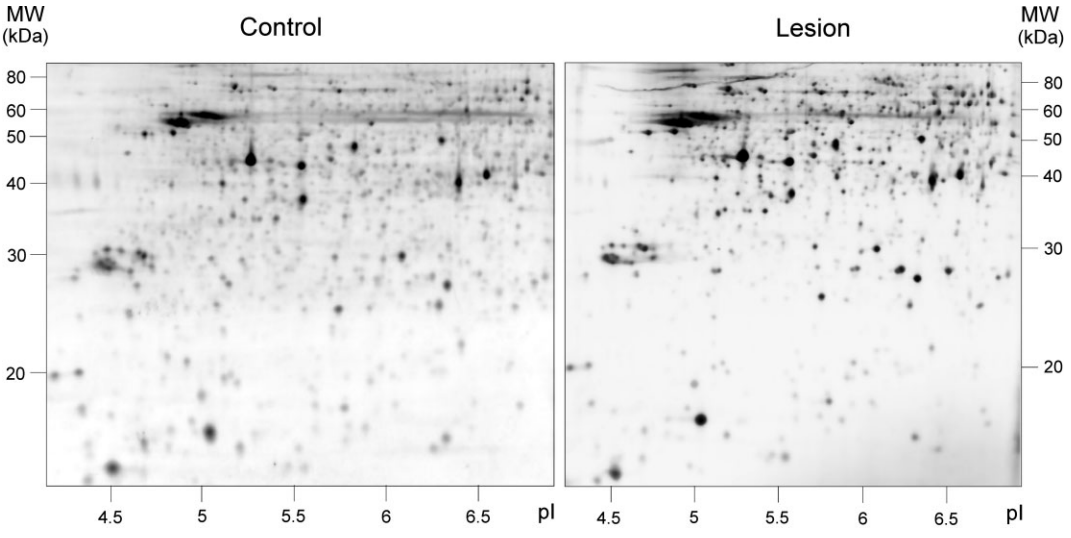

Figure 2. Images of 2-D gels of proteins from the intact corpus cerebelli ("Control") and lesioned corpus cerebelli ("Lesion").

Table 2. Listing of the differentially expressed proteins identified by proteome analysis

Spot number	Protein name	Fold change	M_r (kDa)/p*I*	Number of peptide matches	Peptide sequences	Proposed function	GI number
31700	β-Actin	2.1	42/5.3	5	VAPEEHPVLLTEAPLNPK SYELPDGQVITIGNER GYSFTTTAER QEYDESGPSIVHR AVFPSIVGRPR	Cytoskeletal protein of axons	9049272
32038	β-Tubulin	2.9	50/4.8	6	GHYTEGAELVDSVLDVVR FPGQLNADLR YLTVAAVFR LHFFMPGFAPLTSR ISVYYNEASGGK ISEQFTAMFR	Cytoskeletal protein of axons and endothelial cells	18157542
31730	β1-Tubulin	3.6	50/4.8	1	FPGQLNADLR	Cytoskeletal protein related to neurogenesis	135448
32719	Keratin-10	0.5	59/5.1	2	LKYENEVALR SQYEQLAEQNRK	Intermediate filament protein; negative regulation of cell proliferation	40354192
31559	Chaperonin containing tailless-complex polypeptide 1, subunit ε	2.4	60/5.4	1	ALHDALCVIR	Chaperoning of cytoskeletal proteins	37681753
32035	Tropomodulin-3 and -4	2.3	40/4.7	1	FGYHFTQQGPR	Capping of slow-growing ends of actin filaments	34858039
32711	Bullous pemphigoid antigen 1	4.2	38/6.4	0	–	Linking of actin with intermediate filament proteins	27923959
32500	Myosin heavy chain	2.5	22/5.5	1	LAQESIMDLENDK	Cellular motility of axons	21623523
32258	B2-Lamin	2.9	68/5.4	2	TLYESELADAR LALDMEINAYR	Nuclear assembly during mitosis	228591
31940	78,000-Da glucose-regulated protein	3.7	73/5.0	4	DNHLLGTFDLTGIPPAPR IEIESFFEGEDFSETLTR VTHAVVTVPAYFNDAQR AKFEELNMDLFR	Neuroprotection by reducing apoptotic cell death	4033394
31659	Glutamine synthetase	2.2	42/6.4	1	RPSANCDPFSVTEALIR	Neuroprotection by converting glutamate into glutamine	19923206
32953	Cytosolic aspartate aminotrans-ferase	0.5	47/6.7	1	NFGLYNER	Neuroprotection by reduction of glutamate and aspartate	47522636
32289	α-Enolase	2.0	48/6.2	5	IGAEVYHNLK IVIGMDVAASEFYK AAVPSGASTGIYEALELR SGETEDTFIADLVVGLCTGQIK DATNVGDEGGFAPNILENK	Energy metabolism	1706653
32166	β-Enolase	2.1	47/7.1	2	AAVPSGASTGIYEALELR NGKYDLDFK	Energy metabolism	105934

Table 2. Continued

Spot number	Protein name	Fold change	M_r (kDa)/p*I*	Number of peptide matches	Peptide sequences	Proposed function	GI number
32152	F-ATP synthase β-subunit	2.1	55/5.1	6	AHGGYSVFAGVGER FTQAGSEVSALLGR LVLEVAQHLGENTVR AIAELGIYPAVDPLDSTSR VALVYGQMNEPPGAR VLDTGAPIRIPVGPETLGR	Energy metabolism	5689156
32230	Vacuolar adenosine triphosphatase	2.5	69/5.4	5	ALDEYYDKHFPEFVPLR VGHSELVGEIIR EASIYTGITLSEYFR YSNSDVIIYVGCGER LAEMPADSGYPAYLGAR	Possibly regulation of cellular growth	14915706
32860	Calcineurin	0.4	60/5.6	1	AHEAQDAGYR	Regulation of apoptotic cell death	30354308
33032	70-kDa Heat-shock cognate protein	2.8	71/5.3	5	STAGDTHLGGEDFDNR FELTGIPPAPR DNNLLGKFELTGIPPAPR QTQTFTTYSDNQPGVLIQ-VYEGER ARFEELNADLFR	Protein folding; possibly regulation of development	28569550
31702	Phosphoglycerate kinase	2.1	43/5.9	1	VLNNMEIGTSLYDDEGAK	Glycolysis; modulation of DNA polymerization	11228562
32110	Creatine kinase	2.3	43/5.5	2	GTGGVDTAAVGGVFDISNADR GFCLPPHCSR	Energy metabolism; regulation of cell proliferation	29436540
32845	Bone marrow zinc finger 2	0.4	85/9.7	0	–	Transcriptional regulation	8394033
33081	Regeneration-associated protein 1 (similarities to steroid sensitive gene-1 protein from *Danio rerio*)	4.2	100/9.7	1	VMEEPLDTALIPRLMTFLK	?	16200176
32180	Regeneration-associated protein 2 (similarities to protein CG9699-PG from *Drosophila melanogaster*)	0.4	50/6.2	1	ECTPFAVIGSNTVVEAR	?	41152396

GI number, genInfo identifier of the NCBI

the lesioned CCb relative to the intact CCb varied from −12.4- to +10.2-fold (Fig. 3). Within this range, 204 spots showed a decrease in intensity at least by a factor of −2, whereas 107 spots exhibited an increase in intensity at least by a factor of +2. Out of the latter two populations of protein spots, statistically significant intensity differences were found in 53 spots ($P < 0.05$, *t*-test). Thirty of these spots showed an increase in intensity, whereas 23 spots displayed a decrease. The spots exhibiting these differences were located throughout the 2-D gels, thus covering both small and large molecular weight domains, as well as the entire p*I* range analyzed.

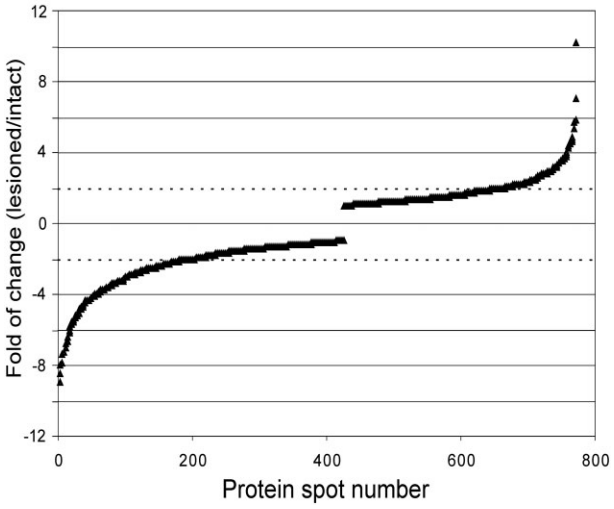

Figure 3. Scatter plot of the fold changes of 772 polypeptide spots in the corpus cerebelli 3 days after the lesion compared to unlesioned controls. Decrease in protein abundance is indicated by negative changes, increase by positive changes. Proteins are sorted in ascending order of the spot intensity change. The analysis is based on a comparison of the averaged spot intensities of four 2-D gels from lesioned brains and three 2-D gels from intact brains. The dotted lines indicate the +2-fold and −2-fold threshold.

3.1.2 Identification of differentially expressed proteins

Identification was accomplished *via* PMF. Protein spots that could not be unambiguously identified through this approach were further examined by MS/MS fragmentation.

Table 2 lists identified protein spots, together with the changes found in the lesioned CCb relative to an equivalent area in the intact CCb. Spot intensity was increased in the following identified proteins after lesioning of CCb: β-actin, β-tubulin, β-1-tubulin, chaperonin containing tailless-complex polypeptide 1 subunit ε, tropomodulin-3 and -4, bullous pemphigoid antigen 1, myosin heavy chain, B2-lamin, 78 000-Da glucose-regulated protein, glutamine synthetase, cytosolic aspartate aminotransferase, α-enolase, β-enolase, F-ATPsynthase β-subunit, vacuolar adenosine triphosphate, 70-kDa heat-shock cognate protein, phosphoglycerate kinase, and creatine kinase. A decrease in spot intensity after application of lesions to CCb was observed in keratin-10, cytosolic aspartase aminotransferase, calcineurin, and bone marrow zinc finger 2. Two proteins, one of which showed an increase and the other a decrease in abundance after cerebellar lesions, did not match any known proteins in the data banks. They were tentatively called "regeneration-associated protein 1" and "regeneration-associated protein 2", respectively.

3.2 Immunological characterization of protein abundance

To verify the protein identification by proteome analysis, and to further characterize the spatiotemporal pattern of protein expression in relation to lesions applied to CCb, two of the identified proteins, β-actin and β-tubulin, were examined through Western blot analysis and immunohistochemistry.

3.2.1 β-Actin

Western blot analysis. The anti-β-actin antibody used in the present study reacted in tissue lysates from the area around the lesion in *Apteronotus leptorhynchus* with a single protein band at approximately 42 kDa as revealed by Western blot analysis (Fig. 4, lane 2). This molecular weight was virtually identical to that of the protein recognized by the same antibody in the lysate from the mouse cerebellum (Fig. 4, lane 3).

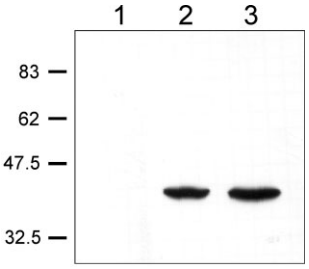

Figure 4. Characterization through Western blotting of the protein recognized by the anti-β-actin antibody. (1) Lysis buffer only, thus serving as a negative control. (2) Lysate from tissue at the area of the lesion, 4 days after application of a lesion to one hemisphere of the corpus cerebelli in *Apteronotus leptorhynchus*. (3) Lysate from mouse cerebellum.

Immunohistochemistry. In the CCb, the anti-β-actin antibody immunostained fibers. These fibers were virtually absent in the intact CCb (Fig. 5A) with the exception of an area at the midline of the CCb-gra, where some were present, which preferentially ran in a dorsoventral direction.

At a survival time of 6 h after lesion, single-labeled fiber fragments were found in the path of the lesion, both within the dorsal molecular layer and in the granular layer. The overall number of these fiber fragments was low but significantly above the numbers in the CCb of intact fish and in the hemisphere contralateral to the site of lesion. The labeled fibers were thin and short (rarely running over more than 10 μm in the transverse plane of sectioning) and exhibited a moderate to high intensity of immunolabeling.

At 1 day after lesion, a dense plexus of intensely labeled fibers had developed (Fig. 5B). This plexus was largely restricted to an area in the vicinity of the lesion in the dorsal molecular layer of CCb. It consisted of two types of fibers: The first type was short and thin, whereas the second was rather long (many could be followed over 20–30 μm) and thick. The latter ran predominantly in the dorsoventral direction.

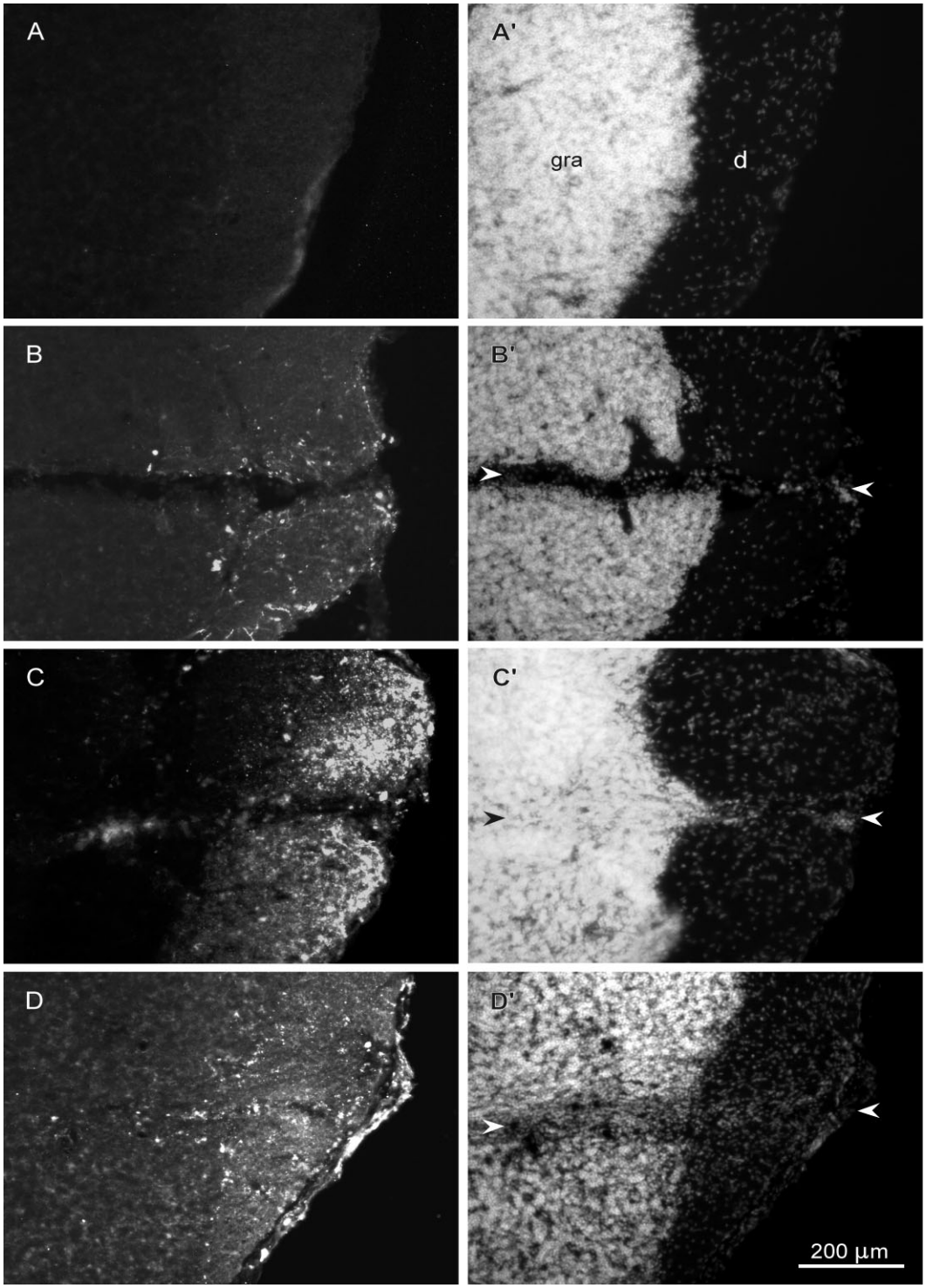

Figure 5. Pattern of immunostaining against β-actin in the intact (A) and injured (B–D) corpus cerebelli of *Apteronotus leptorhynchus*. In the DAPI counterstain of the transverse sections (A'–D'), the right hemisphere is shown with its granular layer (gra) and dorsal molecular layer (d) (dorsal: right; ventral: left; medial: up; lateral: down). The lesion path is indicated by arrowheads. Whereas in the intact corpus cerebelli immunolabeling is virtually absent (A), immunoreactive fibers have developed at 1 day after lesion in the area around the lesion within the dorsal molecular layer (B). At 3 days after lesion, the size of this fiber plexus and the intensity of immunostaining of fibers has increased (C). At 15 days after the lesioning of the cerebellum, both the number and the intensity of immunolabeling has declined compared to the pattern observed at the 3-day survival time.

At 2 days after lesion, the density of the fiber plexus in the dorsal molecular layer had increased further. Moreover, the area occupied by the fibers was much larger, stretching from the path of lesion approximately 300 μm in lateral and medial direction. Both the short thin and the long thick fiber fragments were intensely labeled.

At 3 and 5 days after application of the lesion, the pattern of immunolabeling resembled that after 2 days except that in addition to the fiber plexus in the dorsal molecular layer, there were also fibers present in the CCb-gra (Fig. 5C). However, in contrast to the dorsal plexus, the latter was restricted to the lesion path and an area stretching a few tens of micrometers laterally and medially.

At 10 and 15 days following the lesioning of CCb, β-actin immunoreactivity showed signs of decline (Fig. 5D). Although short thin and long thick fibers were still present, they were not as abundant as found at shorter post-lesion survival times. Furthermore, the fibers were rather weakly labeled.

At 30 days after lesion, the pattern of immunolabeling in the area of the lesion was not significantly different from the labeling in an equivalent region on the contralateral side or in the CCb of non-lesioned fish.

3.2.2 β-Tubulin

Western blot analysis. In Western blots, the anti-β-tubulin antibody reacted in tissue lysates from the area around the lesion in *Apteronotus leptorhynchus* with two protein bands–one at approximately 50 kDa and the other at approximately 30 kDa (Fig. 6, lane 2). In lysates from the mouse cerebellum, the antibody recognized only a single protein band at 50 kDa (Fig. 6, lane 3).

Immunohistochemistry. In the CCb, the anti-β-tubulin antibody used in our investigation immunostained exclusively blood vessels and capillaries (Fig. 7), which formed a rich vascular bed in both the granular and molecular layers. Some of the blood vessels could be followed for up to 100 μm within a section. Profiles of transversely cut blood vessels revealed a circular lumen with diameters of 5–20 μm, surrounded by a thin endothelial cell layer that was thickened in the region where the crescent-shaped nucleus occupied the cytoplasm. Immunolabeled capillaries were much thinner, with diameters of 1–2 μm.

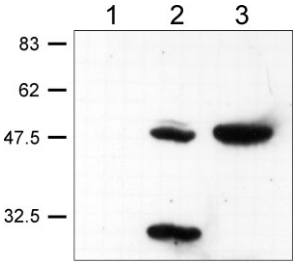

Figure 6. Characterization through Western blotting of the protein recognized by the anti-β-tubulin antibody. (1) Lysis buffer only, thus serving as a negative control. (2) Lysate from tissue at the area of the lesion, 4 days after application of a stab wound to one hemisphere of the corpus cerebelli in *Apteronotus leptorhynchus*. (3) Lysate from mouse cerebellum.

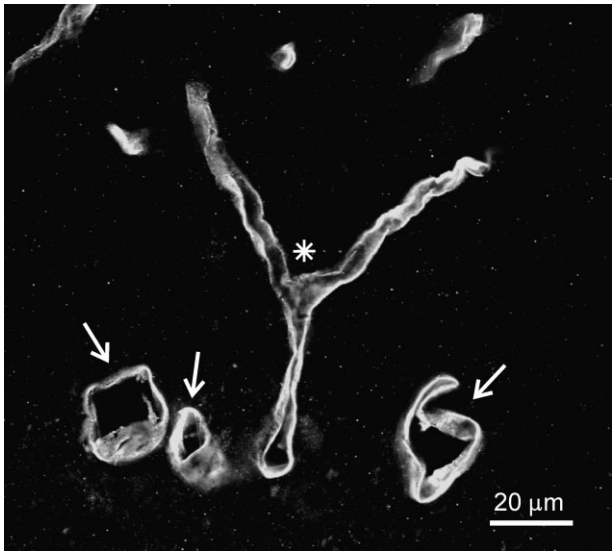

Figure 7. Confocal image of β-tubulin-immunolabeled blood vessels in the corpus cerebelli of *Apteronotus leptorhynchus*. The profiles of these transversely sectioned blood vessels are indicated by arrows. One branching blood vessel that runs largely longitudinally within the optical section is marked by an asterisk.

In the intact CCb, the pattern of immunostaining was dominated by labeling of the larger blood vessels (Fig. 8A). Only a few immunostained capillaries were evident. After lesioning of one hemisphere of the CCb, the spatiotemporal pattern of immunolabeling gradually changed.

At survival times of 6 h and 1 day after lesion, the number and composition of immunopositive blood vessels and capillaries were similar in the area of the lesion as observed in equivalent regions contralaterally or in the intact CCb. However, the intensity of immunolabeling was increased at the lesion site (Fig. 8B).

At 2 days post-lesion survival time, this difference in the intensity of immunolabeling between the area of the lesion and unlesioned regions within the CCb had become more pronounced, whereas no difference was apparent in the number and distribution of immunolabeled structures.

Five days after the lesion, the increase in the intensity of immunolabeling was paralleled by a marked rise in the number of immunopositive vascular structures; the latter was mainly caused by the appearance of many thin capillaries (Fig. 8C).

At post-lesion survival times of 10, 15, and 30 days, a gradual decline in the number of larger blood vessels was found in the area of the lesion, whereas the number of thin capillaries, particularly in the immediate vicinity of the lesion path, remained larger than in other areas of the CCb (Fig. 8D). Furthermore, over the same time period the initi-

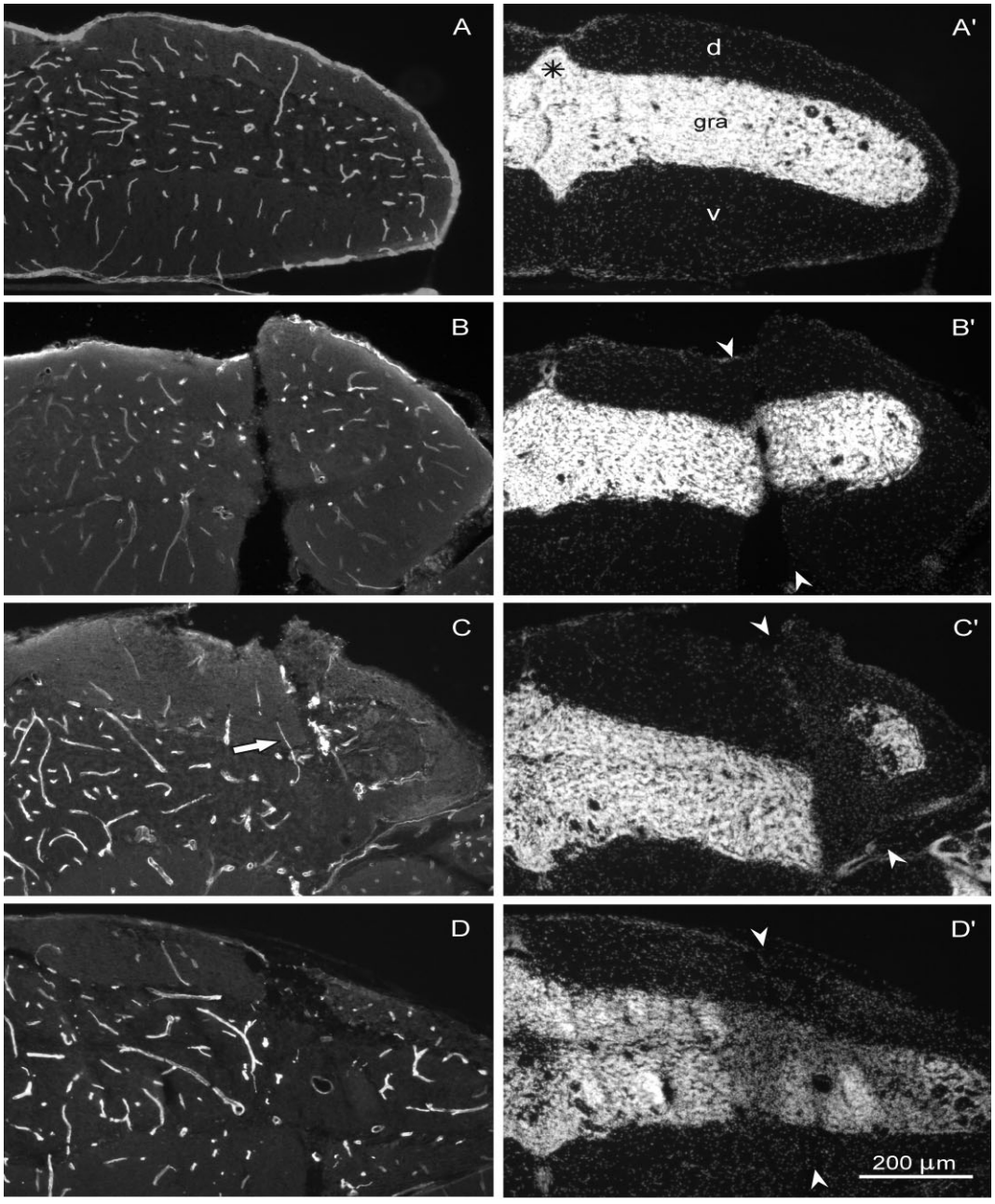

Figure 8. Blood vessels and capillaries immunostained against β-tubulin in the intact (A) and injured (B–D) corpus cerebelli of *Apteronotus leptorhynchus*. In the DAPI counterstain of the transverse sections (A′–D′), the right hemisphere is shown with its granular layer (gra), the dorsal molecular layer (d), and the ventral molecular layer (v) (dorsal: up; ventral: down; medial: left; lateral: right). The "dorsal tip," a protrusion of the granule cell layer into the dorsal molecular layer at the midline, is indicated by * (A′) and the path of the lesion by arrowheads (B′–D′). Whereas in the intact CCb mostly large blood vessels are immunostained, and the intensity of immunolabeling is similar throughout the granular layer and the dorsal molecular layer (A), this pattern changes after application of a lesion (B–D). At 1 day after lesion, an increase in the intensity of immunolabeling is restricted to the area around the lesion (B). At 5 days after lesion, the intensity of immunolabeling remains elevated in the lesion path, but is also increased in other areas of the right hemisphere (C). In addition, the number of thin capillaries is increased in the area of the lesion. At 30 days after lesion, the lesion path and its immediate vicinity has become largely devoid of immunolabeled larger blood vessels, whereas the number of immunolabeled thin capillaries in this area is higher than in the remaining regions of the CCb (D). Two of these thin capillaries are indicated by arrows. Note the restoration of a major part of the granular and molecular layers in the area of the lesion at the latter survival time, as evident through the DAPI counterstain (D′).

ally increased intensity in immunolabel in the area of the lesion gradually returned to the levels evident in the unlesioned hemisphere or in the intact CCb.

4 Discussion

4.1 Methodological considerations

The CCb of *Apteronotus leptorhynchus* is an excellent model system with which to study the cellular mechanisms mediating the enormous regenerative potential of the CNS of teleost fish. Due to the prominent position of this structure (it forms a roof on top of the brain except over the telencephalon), mechanical lesions can readily be applied by puncturing the skull of the anesthetized fish with a sterile surgical blade without damaging other parts of the brain. Guided by landmarks on the fish's head, lesions can be made in a defined way, resulting in an approximately 1-mm-deep cut traveling in a parasagittal direction in the CCb. Furthermore, the major cellular modifications accompanying the regeneration of the injured tissue are well characterized (for reviews, see [3, 4]), thus allowing the investigator to correlate changes in gene expression or protein abundance after the lesion with specific events of the repair process.

By combining this lesion paradigm with proteome analysis, we examined changes in protein abundance after application of mechanical lesions to the CCb. A post-lesion survival time of 3 days was chosen because previous studies have demonstrated its importance especially for the recruitment of newly generated cells replacing the lost ones [13]. At this time point, cell proliferation is dramatically up-regulated, both in areas near the lesion and in proliferation zones of the CCb that continuously generate new cells in intact fish.

Analysis of protein abundance in the area of the lesion relative to that in an equivalent region of unlesioned fish showed that out of almost 900 protein spots identified in 2-D gels, the differential spot intensity was significantly increased, at least twofold, in 30 spots and significantly reduced, at least to half the intensity of control tissue, in 23 spots. The sample preparation protocol employed and the pH range covered only allowed part of the total number of proteins expected to be present in the CCb to be identified. Thus, our finding indicates that a large number of proteins, probably over 100, are potentially involved in regeneration of the injured cerebellar tissue. This demonstrates that a "candidate protein approach", typically based on the selection of single proteins known to play a role in development or regeneration of other systems, is not sufficient to adequately reflect the molecular complexity of the many sub-processes underlying the repair of damaged tissue. Moreover, using this traditional approach, it is extremely cumbersome to identify novel proteins that contribute to the restoration of tissue lost to injury or degenerative disease. As shown by the present investigation, these difficulties can be overcome by proteome analysis.

Out of the 53 proteins whose abundance was significantly altered after lesions, we succeeded in the identification of 24 by PMF and MS/MS fragmentation. Two of the proteins, β-actin and β-tubulin, were further characterized through immunohistochemistry. By variation of the post-lesion survival time and comparison of the immunolabeling with that in the unlesioned hemisphere and the CCb of intact fish, detailed information on the spatiotemporal pattern of protein abundance in the region of the lesion was acquired. Equally important, the immunological identification of the proteins and the observed changes in immunolabeling after lesions provides independent support of the results obtained through the proteome analysis, thus underscoring the power of the latter approach.

4.2 Functional implications of alterations in protein abundance

The functions of most of the proteins identified in the present investigation have been analyzed in other systems and organisms at varying degrees. Such studies involve both neuronal and non-neuronal cells, intact and regenerating tissue, embryonic and adult development, as well as teleostean and non-teleostean species. The discussion of possible functions of individual proteins (see below) is based on this information.

Two proteins identified in our investigation are novel, meaning that no information on possible functions is available. One of these proteins, which we have tentatively termed "regeneration-associated protein 1", exhibits a marked increase in abundance in the injured CCb and is similar to a novel protein identified in zebrafish. The latter protein shows some similarities to the steroid-sensitive gene-1 protein identified previously [18, 19]. The abundance was decreased in the second protein, termed "regeneration-associated protein 2", which shows certain similarities with the novel protein CG9699-PG previously identified in *Drosophila melanogaster.*

4.2.1 β-Actin

Actin, one of the major constituents of the cytoskeleton, is highly conserved between species (for review, see [20]). Together with other cytoskeletal proteins, it provides an intracellular scaffolding of the cell. In addition, actin is involved in cell motility and the transport of intracellular cargos to their destinations, particularly along the axon. One of its three major isoforms, β-actin, is a 42-kDa protein enriched in actively growing structures, or structures with a high capacity for morphological modifications, such as growth cones, filopodia, migrating cell bodies, axonal tracts, and dendritic spines [21–23]. Similarly, regeneration studies have demonstrated an up-regulation of actin within a few days after axotomy, reflecting the emergence of axonal sprouts and the concomitant needs to lengthen the axon shaft and to support membrane expansion at the growth cone [24–26]. Congruent with this finding, induction of axonal sprouting by treatment

of the spinal cord of adult rats with antibodies against the neurite outgrowth inhibitor Nogo-A led to an increased transcription of α-actin [27].

Echoing the results obtained in mammalian systems, our proteome analysis revealed an increase in the abundance of β-actin 3 days after application of the lesion to the teleostean cerebellum. This change in protein abundance was examined in more detail by employing immunohistochemical approaches combined with various survival times after application of the lesions to the CCb. Since the monoclonal antibody used in these experiments is directed against a conserved β-cytoplasmic actin N-terminal peptide, and Western blot analysis showed virtually identical protein bands in lysates from fish and mouse cerebellum, we assume that this antibody detects a fish ortholog of β-actin in the CCb of *Apteronotus leptorhynchus*.

As shown by the immunohistochemical experiments, an increase in β-actin immunoreactivity is detectable as early as a few hours following injury. A decline is observed 10–15 days after lesion. We suggest that the increase in abundance of β-actin over the time span of approximately 2 weeks is associated with the regeneration of injured axons and the development of axons of the newly generated cells.

4.2.2 β-Tubulin and β1-tubulin

Tubulin, the principal component of microtubules, is a heterodimer of two closely related proteins, α- and β-tubulin, each with an M_r of approximately 50 kDa. Both the α- and β- subunit consist of a family of homologous isoforms, which appear to be related to different microtubule functions.

The results of our proteome analysis have demonstrated increases in abundance of both β-tubulin and one specific isoform of this subunit, β1-tubulin, 3 days after application of lesions to the CCb. This does not exclude regeneration-associated changes in abundance of other isoforms, especially of α-tubulin, which occur in stoichiometric amounts with β-tubulin in microtubules. Regeneration-associated changes in the expression of tubulin have been examined in a variety of systems. These studies have shown that in systems that exhibit spontaneous regeneration, regrowth of axons is accompanied by up-regulation of specific isoforms of tubulin. Such systems include the peripheral nervous system of mammals [26, 28, 29] and the optic nerves of fish and amphibians [30, 31]. Conversely, in the CNS of mammals, which lacks the potential for axonal regeneration, mRNAs for tubulin are decreased and remain low after axotomy [26, 32–35]. This comparison suggests that the increase in abundance of β-tubulin after lesioning of the CCb may be related to the regrowth of injured axons, or the development of axons of newly generated cells. Thus, the changes in β-tubulin abundance appear to be closely related to the changes observed in β-actin abundance (see previous sections).

The increase in the abundance of a protein resembling the human form of β1-tubulin in *Apteronotus leptorhynchus* during regeneration points to the possibility of an additional function. In zebrafish, β1-tubulin has been shown to be restricted to regions in the peripheral and CNS that are abundant with early differentiating neurons during embryonic development [36]. In adult zebrafish, this expression is confined to a subset of proliferative zones in various regions of the brain and the olfactory epithelium. Thus, the increase in β1-tubulin abundance in the regenerating CCb could be related to neurogenesis.

The results of the immunohistochemical experiments are intriguing in that the anti-β-tubulin antibody employed immunoreacted exclusively with endothelial cells in the CCb. It is unclear whether the absence of labeling of other cerebellar cell types is related to the occurrence of a second protein band, in addition to the one at 50 kDa, at approximately 30 kDa in Western blots. Such an additional band has not been described in mammalian systems. However, anti-β-tubulin antibodies are widely used to label endothelial cells in mammalian tissue, in addition to other cell types.

The pattern of immunolabeling of the cerebellar endothelial cells suggests two major processes following application of a lesion: First, the blood vessels in the area of the lesion undergo cell death within a few weeks after the injury. Second, the depletion of large blood vessels is paralleled by a repopulation of the lesion area by thin capillaries, possibly due to angiogenesis. Since the latter aspect is often neglected in studies of regeneration of the CNS, it would be interesting to address the possibility of generation of new endothelial cells induced by injury in future investigations.

4.2.3 Keratin-10

Keratins are members of the intermediate filament gene family [37] and form the main components of the intermediate filament cytoskeleton in epithelial cells. They include approximately 30 different polypeptides that are expressed in a cell type-specific and differentiation-specific manner. Among them, keratin-10 (K10) is unique because its expression is restricted to post-mitotic cells [38]. Like other keratins, one of its major functions is to confer mechanical stability to the epidermis. An additional role in the regulation of cell proliferation has been suggested following examination of K10-null mice. In these animals, the keratinocytes in the basal layer exhibit hyperproliferation, presumably induced by neighboring keratinocytes in the suprabasal layer through transmission of a paracrine signal [39]. Under the influence of hyperproliferative stimuli, such as those that act during wound healing or in cancer, the expression of K10 is dramatically down-regulated [40–44]. Similarly, forced expression of K10 inhibits cell proliferation both *in vitro* [45] and *in vivo* [46]. Taken together, these observations suggest a negative involvement of K10 in the regulation of keratinocyte proliferation.

In the present study, the identification of K10 in the cerebellum of *Apteronotus leptorhynchus* was somewhat surprising because expression of this keratin type in the CNS has not been previously reported. However, zebrafish

orthologs of the human keratin types K8 and K18, also originally thought to be absent from the CNS, were recently identified in various structures of the retina, brain, and spinal cord [47]. Based on the decrease in abundance of K10 in the lesioned CCb 3 days after lesion (*i.e.*, when cell proliferation is several-fold higher than in the intact CCb [13]), this keratin type may exert a similar function as proposed for the epidermis–negative regulation of cell proliferation. The increase in cell proliferation at this time point is accompanied by a marked increase in the expression of activin, a member of the TGF-β superfamily (G. K. H. Zupanc and S. Werner, unpublished observations). Notably, members of the latter molecular class act in a paracrine-like fashion and have been suggested as candidates mediating the proliferation-regulating effect of K10 [39]. Based on these results, it will be important to identify the cell type(s) expressing K10 in both the intact and the injured teleostean cerebellum and to investigate their relationship with the proliferating cells during regeneration.

4.2.4 B2-Lamin

Lamins belong to the family of intermediate-filament proteins and are an essential component of the nuclear lamina, a protein meshwork located between the inner nuclear membrane and the peripheral chromatin. Among others, they exert important functions for the maintenance of the nuclear morphology and the disassembly and reassembly of the nuclear envelope during mitosis (for review, see [48]). Based on their primary sequence, expression pattern, and biochemical properties, lamins are classified as either A-type or B-type. Whereas A-lamins are predominantly expressed in differentiated cells, B-type lamins are typically associated with membranes during mitosis.

The latter association is in agreement with the observed increase in the abundance of B2-lamin 3 days after application of a mechanical lesion to the CCb. As mentioned before, at this post-lesion survival time, the number of S-phase cells in the CCb is dramatically increased compared to control animals [13]. We, therefore, propose that B2-lamin is functionally involved in nuclear assembly during mitosis of the new cells generated in response to injury in the adult teleostean cerebellum.

4.2.5 Myosin heavy chain

Myosins form a superfamily of molecular motors that are biochemically defined as actin-activated Mg^{2+}-ATPases. Besides their involvement in muscle fiber contraction, several classes of non-muscular myosin are expressed in the nervous system and have been implicated in various aspects of cellular motility in the developing nervous system (for review, see [49]). In particular, isoforms of class II, which are composed of one pair of heavy chains and two pairs of light chains, have been shown to be involved in the outgrowth and retraction of neuritic processes [50, 51], lamellipodial protrusion and thus growth cone motility [52], and migration of distinct groups of neurons [53].

The up-regulation in the lesioned fish cerebellum of a protein homologous to the myosin heavy chain from the skeletal muscle of Chum salmon, *Oncorhynchus keta* [54], adds an important aspect to this list of functions because it suggests an involvement of myosin in the regeneration of the nervous system. Since in *Apteronotus leptorhynchus* the first new cells that migrate from the proliferation zones in the cerebellum arrive at the site of lesion only approximately 10 days after the lesion [14], it is unlikely that myosin is primarily involved in cellular migration at the time point examined, 3 days after lesion. Rather, we hypothesize that non-muscular isoforms of myosin participate during this early stage of brain repair in axonal regeneration, including neurite outgrowth and growth-cone mediated axonal pathfinding.

4.2.6 Chaperonin containing tailless-complex polypeptide 1, subunit ε

The chaperonin containing tailless-complex polypeptide 1 (TCP1), commonly referred to as CCT, is a cytosolic heterooligomeric chaperonin promoting the folding of cytoskeletal components, particularly newly synthesized α- and β-tubulin [55] and denaturated actin [56] in an ATP-dependent process. Thus, it is expressed especially during events in which the cytoskeleton undergoes extensive remodeling, such as neuritogenesis and mitotic spindle formation. It is likely that similar functions are associated with the up-regulation of CCT observed in the present study 3 days after lesion. We, therefore, hypothesize that the up-regulation of CCT is causally linked to the up-regulation of β-actin and β-tubulin and that CCT provides molecular chaperoning to these cytoskeletal constituents. There is indication that CCTs consist of a heterogeneous population differing in the relative abundance of the various subunits. In addition, the intracellular distribution of the CCTα population is somewhat different from the CCTβ, CCTγ, and CCTε components, possibly reflecting specialization of chaperonin function in different cytoplasmic compartments of a neuron [57]. Because of the latter two observations, it will be interesting to examine whether the up-regulation of CCT is restricted to CCTs containing the ε component.

4.2.7 Tropomodulin

Tropomodulins are a family of proteins whose sole function appears to be to cap the slow-growing (pointed) ends of actin filaments [58, 59] (for review, see [60]). In vertebrates, four canonical isoforms, conserved across species, have been described. By blocking the association and dissociation of actin monomers, tropomodulins exert control of the lengths and dynamics of actin filaments.

So far, nothing is known about the involvement of tropomodulins in regeneration. The up-regulation of proteins similar to the mammalian tropomodulin classes 3 and 4 in the lesioned cerebellum of *Apteronotus leptorhynchus* could simply reflect the increase in actin at the examined time of survival and thus the need to provide sufficient amounts of tropomodulin to negatively regulate actin filament assembly. Furthermore, as tropomodulin-3 has been shown to negatively regulate cell motility in endothelial cells [61], the up-regulation of its homologous protein in fish could also lead to a decrease in the degree of cell migration. Indeed, there is evidence that cells generated in more distant proliferation zones (such as the one at the midline in the dorsal molecular layer of CCb) start migrating to the site of lesion only at roughly 10 days after lesion. The onset of this migratory activity, as well as the pattern of migration, appear to be largely determined by the presence of radial glial fibers, which are detectable in the ipsilateral molecular layer of the CCb approximately 2 days earlier [14]. It remains to be examined whether or not tropomodulin also negatively regulates the cellular motility of these new cells.

4.2.8 Bullous pemphigoid antigen 1

Bullous pemphigoid antigen 1 (BPAG1), first identified with antisera from patients with the autoimmune disorder bullous pemphigoid, is a member of the rather small plakin family. The neuronal isoforms of BPAG1 contain, at opposite ends of its coiled-coil rod domain, actin- and neurofilament-binding sites through which these cytoskeletal proteins exert a key role in linking actin and neuronal intermediate filaments [62, 63]. In BPAG1-null mice, the failure to tether neurofilaments to the actin cytoskeleton results in a markedly perturbed axonal architecture [63].

Although the role of BPAG1 in neuronal development has not yet been examined in detail, it appears reasonable to assume that this protein plays an important role in the organization of the cytoskeleton of newly generated neurons. This hypothesis is consistent with the observed increase in the abundance of BPAG1 3 days after lesioning of the CCb, at a time point when the rate of cell production (and thus the formation of the cellular cytoskeleton) is markedly up-regulated [13]. The rise in BPAG1 abundance is paralleled by an increase in the amount of one of its potential binding partners, β-actin (see above).

4.2.9 78 000-Da glucose-regulated protein

The 78 000-Da glucose-regulated protein (GRP-78), identical to the immunoglobulin heavy-chain-binding protein, belongs to the heat-shock protein-70 family (HSP-70). It is a resident protein of the ER, believed to act as a chaperone by binding to misfolded proteins to prevent intramolecular and intermolecular aggregation (for reviews, see [64–66]). Overexpression of proteins of the HSP-70 family has revealed cytoprotective properties against various injuries in many different cell types (for review, see [67]). In the rodent brain, expression of GRP-78 is up-regulated after kainic acid-induced seizures both during adulthood [68] and during early post-natal development [69]. Similarly, during sleep deprivation, GRP-78 mRNA levels are elevated in several brain regions, an effect thought to reflect a neuroprotective response to prolonged wakefulness [70].

It is possible that the teleostean ortholog of GRP-78 exerts a similar neuroprotective function, as indicated by the elevated protein level 3 days after lesioning of the CCb. Specifically, this effect could be mediated by reducing apoptotic cell death. Such a role has been suggested by research on transgenic mice that overexpress HSP-70 after ischemia and seizures [71] and is compatible with the time course of apoptotic cell death after application of cerebellar lesions in *Apteronotus leptorhynchus* [5]. In the latter system, peak levels of apoptosis are observed between 30 min and 24 h after lesion. After the latter time point, the number of cells undergoing apoptotic cell death rapidly declines.

4.2.10 Glutamine synthetase

Glutamine synthetase is a glia-specific enzyme that converts synaptically released glutamate into the non-toxic amino acid glutamine. Under normal conditions, this mechanism prevents the accumulation of neurotoxic amounts of glutamate in neural tissue and thus protects neurons from cell death. However, under traumatic conditions the amount of glutamine synthetase is insufficient to catalyze the excessive amounts of glutamate released by damaged cells. Thus, this mechanism fails to limit the spreading of the damage caused by the continuous overexcitation of post-synaptic glutamate receptors. Moreover, the occurrence of injury, focal ischemia, and a number of neurological disorders is often accompanied by a decline in the expression of glutamate synthetase [72–77], thereby aggravating the effect of neurodegeneration induced by glutamate neurotoxicity.

Considering the down-regulation of glutamine synthetase under traumatic conditions in the mammalian CNS, the increase in the abundance of glutamine synthetase in the fish cerebellum after a mechanical lesion is particularly remarkable. It is likely that this difference is causally linked to the difference between the two taxa in the extent of neural cell death after traumatic injury. Indeed, in cultures of mammalian retinal explants elevation of glutamine synthetase in glial cells by induction of the endogenous gene, or exogenous supply of the purified enzyme, can protect cells against neural degeneration [78].

4.2.11 Cytosolic aspartate aminotransferase

Cytosolic aspartate aminotransferase is one of the key enzymes of the malate-aspartate shuttle and exerts a number of tissue-specific functions. In the brain, this includes the catalytic amino group transfer from glutamate or aspartate to a keto acid acceptor–oxaloacetate or α-ketoglutamate, respec-

tively. Treatment of cultured astrocytes or neurons with an inhibitor of aspartate aminotransferase leads to a decrease of both astrocytic and neuronal glutamate [79]. Along similar lines, reduced levels of aspartate aminotransferase are thought to account for the reduced concentration of aspartate and glutamate in the brain of humans with Down's syndrome [80].

Assuming a similar relationship in the fish cerebellum, the reduced level of aspartate aminotransferase in the CCb after stab-wound lesions could result in a reduction of glutamate and potentially aspartate as well. Such an effect would supplement the proposed reduction of glutamate by the observed increase in the level of glutamine synthetase (see above). Thus, each of the two mechanisms would prevent the accumulation of neurotoxic amounts of glutamate, thereby protecting the neurons from cell death.

4.2.12 α- and β-Enolase

Enolase (2-phospho-D-glycerate hydrolase) is an essential enzyme of the glycolytic pathway, which catalyzes the reversible dehydration of 2-phospho-D-glycerate to the high-energy phosphoenolpyruvate. The functional enzyme is a homodimer or heterodimer composed of two out of the three different subunits termed α, β, and γ. The αα homodimer is found predominantly in immature cells but also in mature cells of many types of tissue, including the brain tissue. In other cells of the nervous system, a switch to the αγ and γγ forms occurs during ontogenesis. Although the latter homodimer is called neuron-specific enolase, expression of this isoform has also been found in glial cells (for review, see [81].

Whereas the sequences of the α- and β-subunits are well characterized in several fishes, to our knowledge the sequence of the γ-subunit has not yet been determined in any fish species. Thus, while in our study one of the two isoforms could be unambiguously identified as an α-enolase, the identity of the other, which is most similar to human β-enolase, is less clear. One possibility is that the second protein represents a fish-specific form of β-enolase. This, however, appears unlikely because β-isoforms have been found only in muscles and never in the nervous system of any vertebrate species. Alternatively, the second isoform could correspond to an enolase containing the γ subunit. This explanation appears plausible because, among the three subunits, the genes encoding the β- and γ-form have been proposed to be most closely related [82]. However, final clarification of this issue will have to await the availability of information on the complete sequence of a γ-enolase from the nervous system of fish. Until then, we will tentatively designate the new protein as "fish brain enolase related to human β-enolase".

The protein levels of both the α-enolase and the "fish brain enolase related to human β-enolase" were higher in the injured CCb of *Apteronotus leptorhynchus,* than in the intact. A similar injury-related effect has been observed in the mammalian brain: In cultures of cerebellar cells, mechanical trauma causes an elevated release of neuron-specific enolase [83]. In the forebrain, the transformation of astrocytes from the normal resting stage to a reactive stage is accompanied by the expression of neuron-specific enolase [84]. Such increases in enolase abundance could reflect a higher metabolic demand of cells during brain repair. In addition and as suggested by a number of *in vitro* studies, enolase (probably of the γγ homodimeric form) could act as a neurotrophic factor that promotes survival of neurons [85–87].

4.2.13 F-ATP synthase β-subunit

F-ATP synthase, an ubiquitous and highly conserved enzyme, is located in the inner membrane of mitochondria and catalyzes the formation of ATP from ADP and phosphate. It consists of two major portions: a membrane domain, F_0, comprising α-, β-, γ-, δ-, and ε-subunits; and a soluble domain, F_1, composed of a-, b-, and c-subunits (for review, see [88].

To our knowledge, the increase in the abundance of the β-subunit of F-ATP synthase after cerebellar lesions found in the present study is the first reported indication of a possible involvement of this enzyme in the process of regeneration of the nervous system. This increase is not surprising considering the anticipated rise in energy demand associated with tissue repair. One candidate potentially mediating the up-regulation of F-ATP synthase is nerve growth factor (NGF), as suggested by the following two observations. First, numerous studies demonstrate that NGF and its receptors are rapidly and markedly up-regulated after traumatic brain injury (for review, see [89]). Second, in cultured adult rat dorsal root ganglion neurons, mRNA encoding F-ATP synthase β-subunit is rapidly induced by this neurotrophic factor [90].

4.2.14 Vacuolar adenosine triphosphatase

Vacuolar adenosine triposphatases (V-ATPases) are multisubunit enzymes found in membranes of many acidified organelles (for review, see [91]). By translocating protons across the membrane, they mediate regulation of pH and generation of electrochemical gradients in the intracellular compartments. Sequence analysis has revealed a high degree of similarity with F-ATPases (see Section 4.2.13), suggesting the evolution of the two proteins from the same enzyme [92]. V-ATPases are involved in various functions, including protein sorting, receptor-mediated endocytosis, and neurotransmitter uptake. Increasing evidence also suggests that it has an important role in cell proliferation, as inhibition of V-ATPases suppresses growth in various cell types [93–96].

This latter function may also be exerted by the V-ATPase identified in the cerebellum of *Apteronotus leptorhynchus.* Such a notion is compatible with the observed increase in abundance of this enzyme at a time point when the production of new cells recruited for later replacement of damaged cells is dramatically up-regulated [13].

4.2.15 Calcineurin

Calcineurin is a Ca^{2+}/calmodulin-dependent serine/threonine protein phosphatase that participates in a number of cellular processes and Ca^{2+}-dependent signal transduction pathways. Among its functions, it acts as an essential component in signaling cell death. This function is mediated by interaction of calcineurin with BAD, a pro-apoptotic member of the Bcl-2 family. Under non-apoptotic conditions BAD is maintained in its inactive phosphorylated state by certain serine-threonine kinases, whereas in the presence of apoptotic stimuli BAD is dephosphorylated by calcineurin and translocated from the cytosol to the mitochondria. This leads to an inhibition by BAD of Bcl-2 and Bcl-x_L, two anti-apoptotic members of the Bcl-2 family of proteins, thus promoting apoptosis [97] (for review, see [98]).

In the mammalian CNS, neurons and oligodendroglia can be protected from cell death induced by ischemia or traumatic injury through specific inhibitors of calcineurin, such as the immunosuppressant FK506 [99–101]. In fish, cell death induced by brain injury is restricted to the lesion site and areas in the immediate vicinity, as well as to time periods shortly after the injury occurs [5]. The prevention of cell death in larger areas around the lesion site and during time periods beyond the first few days following the injury may be achieved by endogenous activation of a mechanism reminiscent of the one protecting cells from death after administration of FK506 or other inhibitors of calcineurin in mammals. This hypothesis receives support from the fact that the pathway regulating apoptosis is highly conserved among eukaryotes and from the finding of the present study that calcineurin is markedly down-regulated 3 days after application of a mechanical lesion to the cerebellum.

4.2.16 70-kDa Heat-shock cognate protein

The 70-kDa heat-shock cognate protein, a member of the 70-kDa family of heat-shock proteins, is highly conserved among species. Although the level of transcript expression can be up-regulated after sudden increases in temperature, this protein is also constitutively expressed at normal temperature. It is involved in a number of cellular processes, including *de novo* protein folding, translocation of proteins from the endocytic and secretory pathways to the endosomal system, formation and disassembly of protein complexes, and degradation of misfolded proteins (for reviews, see [102, 103]). In addition, the 70-kDa heat-shock cognate protein has been proposed to play a role in development, as indicated by a marked up-regulation of its expression in neuroectoderm/mesoderm-derived structures after gastrulation [104, 105]. It is possible that the latter function is also exerted during the development of new cells produced in response to injury in the cerebellum of *Apteronotus leptorhynchus*. The proposal of such a function is in agreement with the increase in abundance of this protein 3 days after application of the lesion in the CCb. Further studies will be required to specify this developmental role in both the intact and the injured CNS.

4.2.17 Phosphoglycerate kinase

Phosphoglycerate kinase, a major enzyme of the glycolytic (Embden–Meyerhof) pathway, catalyzes the reversible conversion of 1,3-diphosphoglycerate to 3-phosphoglycerate, thereby generating one molecule of ATP. In addition to this well-established role, phosphoglycerate kinase has been shown to reside in cell nuclei and to modulate DNA polymerases, thus influencing DNA replication and repair [106, 107]. The increase in the abundance of phosphoglycerate kinase 3 days after application of the lesion to the CCb could, thus, be causally linked not only to the higher glycolytic demand of the cells during regeneration but also to the rise in the rate of cell proliferation previously demonstrated [13].

4.2.18 Creatine kinase

Creatine kinase, a member of the family of guanidino kinases, is specifically located in cells with high and fluctuating energy requirements. This enzyme plays a crucial role in the regeneration of ATP by catalyzing the reversible transfer of a phosphoryl group from phosphocreatine to MgATP. Increased levels of creatine kinase are found in the cerebrospinal fluid and serum of patients after head injuries. In addition, high activities of creatine kinase correlate with poor prognosis in human patients [108–110]. Similarly, immediately after wounding of murine skin, brain-type cytosolic creatine kinase is transiently up-regulated [111].

Little is known about possible functions of creatine kinase in the process of tissue regeneration. In the liver, which normally does not contain creatine kinase, expression of the brain-type cytosolic isoform leads to improved regeneration in transgenic mice, compared to normal liver, by increasing the rate of cell production [112]. To our knowledge, the possibility of such an effect has not yet been examined during brain regeneration. However, our finding of an increase in creatine kinase in cerebellar tissue in the immediate vicinity of the lesion at 3 days after lesion, when cell proliferation is substantially up-regulated, is compatible with the possibility that this enzyme is not only involved in the general energy metabolism, but may also play a more direct role in the control of cell growth.

4.2.19 Bone marrow zinc finger 2

Bone marrow zinc finger 2 (BMZF2), also referred to as ZNF255, was first identified from a screen of zinc finger proteins expressed in the hematopoietic system [113]. This protein is characterized by the presence of 18 zinc finger

repeats at the C terminus and a domain of approximately 81 amino acids at the N terminus related to a sequence found in the *Krüppel* protein of *Drosophila*, hence called the *Krüppel*-related novel box (KRNB). The finger-like structure of the zinc finger domain is stabilized by a centrally located zinc ion that is coordinated by two cysteines and two histidines.

Although little is known about the expression pattern and the function of this member of the zinc finger gene family, its molecular structure and some experimental evidence suggest that it acts as a transcriptional regulator. Such evidence includes studies on Wilms' tumor, a pediatric kidney cancer. As has been shown, BMZF2 associates with Wilms' tumor suppressor, another zinc finger protein, and inhibits the transcriptional activity of the latter [114]. Nothing is known about its role in the nervous system. To our knowledge, the present study provides the first indication of an expression of the gene encoding BMZF2 in the brain and of a possible role in the process of regeneration. Since transcription factors function as master regulators of "downstream" proteins, further examination of BMZF2 is likely to lead to new insights into the "upstream" mechanisms controlling the regeneration of brain tissue.

In conclusion, proteomics allows for a large-scale identification of proteins involved in regeneration of the CNS. In the present study, we succeeded in the identification of 24 novel protein candidates that participate in the regenerative processes underlying repair of the CCb in *Apteronotus leptorhynchus*. This list includes: cytoskeletal proteins essential for the formation of new cells and proteins mediating the correct assembly of these structural proteins; proteins putatively involved in cell proliferation, cellular motility, neuroprotection, and energy metabolism; and one protein, bone marrow zinc finger 2, that may regulate the transcription of genes of other proteins and thus could act as a master regulator of the repair process.

The identification of a number of proteins previously unknown to be expressed in the vertebrate brain, or to be involved in regeneration of the CNS of any vertebrate species, has important implications, as comparative analysis has demonstrated that the cellular mechanisms underlying axonal and neuronal regeneration are very similar among different taxa. Thus, it is likely that our list includes proteins that also play a role in the regeneration of the mammalian nervous system. Most importantly, however, such a comparative approach is likely to enable investigators to reveal the cellular basis of the enormous difference between fish and mammals in their regenerative potential and thus to define new therapeutic strategies to overcome the limits of the mammalian brain.

We thank Daniela Meissner for her assistance in preparing the figures, and Angie Nichols for her comments on a previous version of the manuscript. This study was funded through grants from the International University Bremen and the Wellcome Trust to G.K.H.Z.

5 References

[1] Larner, A. J., Johnson, A. R., Keynes, R. J., *Biol. Rev.* 1995, *70*, 597–619.

[2] Waxman, S. G., Anderson, M. J., in: Bullock, T. H., Heiligenberg, W. (Eds.), *Electroreception*, John Wiley, New York 1986, pp. 183–208.

[3] Zupanc, G. K. H., *J. Exp. Biol.* 1999, *202*, 1435–1446.

[4] Zupanc, G. K. H., *Brain Behav. Evol.* 2001, *58*, 250–275.

[5] Zupanc, G. K. H., Kompass, K. S., Horschke, I., Ott, R., Schwarz, H., *Exp. Neurol.* 1998, *152*, 221–230.

[6] Kerr, J. F. R., Searle, J., Harmon, B. V., Bishop, C. J., in: Potten, C. S. (Ed.), *Perspectives on Mammalian Cell Death*, Oxford University Press,Oxford 1987, pp. 93–128.

[7] Beattie, M. S., Farooqui, A. A., Bresnahan, J. C., *J. Neurotrauma* 2000, *17*, 915–925.

[8] Vajda, F. J., *J. Clin. Neurosci.* 2002, *9*, 4–8.

[9] Zupanc, G. K. H., Clint, S. C., Takimoto, N., Hughes, A. T. *et al.*, *Brain Behav. Evol.* 2003, *62*, 31–42.

[10] Zupanc, G. K. H., Hinsch, K., Gage, F. H., *J. Comp. Neurol.* 2005, *488*, 290–319.

[11] Zupanc, G. K. H., Horschke, I., *J. Comp. Neurol.* 1995, *353*, 213–233.

[12] Zupanc, G. K. H., Horschke, I., Ott, R., Rascher, G. B., *J. Comp. Neurol.* 1996, *370*, 443–464.

[13] Zupanc, G. K. H., Ott, R., *Exp. Neurol.* 1999, *160*, 78–87.

[14] Clint, S. C., Zupanc, G. K. H., *Dev. Brain. Res.* 2001, *130*, 15–23.

[15] Clint, S. C., Zupanc, G. K. H., *NeuroReport* 2002, *13*, 317–320.

[16] Laemmli, U. K., *Nature* 1970, *227*, 680–685.

[17] Zupanc, G. K. H., *Brain Res. Prot.* 1998, *3*, 37–51.

[18] Marcantonio, D., Chalifour, L. E., Alaoui-Jamali, M. A., Alpert, L., Huynh, H. T., *Endocrinology* 2001, *142*, 2409–2418.

[19] Marcantonio, D., Chalifour, L. E., Alaoui-Jamali, M. A., Huynh, H. T., *J. Mol. Endocrinol.* 2001, *26*, 175–184.

[20] Schoenenberger, C.-A., Steinmetz, M. O., Stoffler, D., Mandinova, A., Aebi, U., *Microsc. Res. Tech.* 1999, *47*, 38–50.

[21] Bassell, G. J., Zhang, H., Byrd, A. L., Femino, A. M. *et al.*, *J. Neurosci.* 1998, *18*, 251–265.

[22] Kaech, S., Fischer, M., Doll, T., Matus, A., *J. Neurosci.* 1997, *17*, 9565–9572.

[23] Micheva, K. D., Vallée, A., Beaulieu, C., Herman, I. M., Leclerc, N., *Eur. J. Neurosci.* 1998, *10*, 3785–3798.

[24] Lund, L. M., Machado, V. M., McQuarrie, I. G., *Exp. Neurol.* 2002, *178*, 306–312.

[25] Lund, L. M., McQuarrie, I. G., *J. Neurobiol.* 1996, *31*, 476–486.

[26] Tetzlaff, W., Alexander, S. W., Miller, F. D., Bisby, M. A., *J. Neurosci.* 1991, *11*, 2528–2544.

[27] Bareyre, F. M., Haudenschild, B., Schwab, M. E., *J. Neurosci.* 2002, *22*, 7097–7110.

[28] Hoffman, P. N., Cleveland, D. W., *Proc. Natl. Acad. Sci. USA* 1988, *85*, 4530–4533.

[29] Miller, F. D., Tetzlaff, W., Bisby, M. A., Fawcett, J. W., Milner, R. J., *J. Neurosci.* 1989, *9*, 1452–1463.

[30] Hieber, V., Dai, X., Foreman, M., Goldman, D., *J. Neurobiol.* 1998, *37*, 429–440.

[31] Mizobuchi, T., Yagi, Y., Mizuno, A., *J. Neurochem.* 1990, *55*, 54–59.

[32] Fournier, A. E., McKerracher, L., *Biochem. Cell Biol.* 1995, *73*, 659–664.

[33] McKerracher, L., Essagian, C., Aguayo, A. J., *J. Neurosci.* 1993, *13*, 2617–2626.

[34] McKerracher, L., Essagian, C., Aguayo, A. J., *J. Neurosci.* 1993, *13*, 5294–5300.

[35] Mikucki, S. A., Oblinger, M. M., *J. Neurosci. Res.* 1991, *30*, 213–225.

[36] Oehlmann, V. D., Berger, S., Sterner, C., Korsching, S. I., *Gene Expr. Patterns* 2004, *4*, 191–198.

[37] Hesse, M., Magin, T. M., Weber, K., *J. Cell Sci.* 2001, *114*, 2569–2575.

[38] Moll, R., Franke, W. W., Schiller, D. L., Geiger, B., Krepler, R., *Cell* 1982, *31*, 11–24.

[39] Reichelt, J., Magin, T. M., *J. Cell Sci.* 2002, *115*, 2639–2650.

[40] Ivanyi, D., Ansink, A., Mooi, W. J., de Kraker, N. W., Heintz, A. P. M., *Differentiation* 1989, *42*, 124–129.

[41] Maddox, P., Sasieni, P., Szarewski, A., Anderson, M., Hanby, A., *J. Clin. Pathol.* 1999, *52*, 41–46.

[42] Roop, D. R., Krieg, T. M., Mehrel, T., Cheng, C. K., Yuspa, S. H., *Cancer Res.* 1988, *48*, 3245–3252.

[43] Toftgard, R., Yuspa, S. H., Roop, D. R., *Cancer Res.* 1985, *45*, 5845–5850.

[44] Winter, H., Schweizer, J., Goerttler, K., *Arch. Dermatol. Res.* 1983, *275*, 27–34.

[45] Paramio, J. M., Casanova, M. L., Segrelles, C., Mittnacht, S. *et al.*, *Mol. Cell Biol.* 1999, *19*, 3086–3094.

[46] Santos, M., Paramio, J. M., Bravo, A., Ramirez, A., Jorcano, J. L., *J. Biol. Chem.* 2002, *277*, 19122–19130.

[47] Schaffeld, M., Knappe, M., Hunzinger, C., Markl, J., *Differentiation* 2003, *71*, 73–82.

[48] Mattout-Drubezki, A., Gruenbaum, Y., *Cell. Mol. Life Sci.* 2003, *60*, 2053–2063.

[49] Brown, M. E., Bridgman, P. C., *J. Neurobiol.* 2004, *58*, 118–130.

[50] Wylie, S. R., Chantler, P. D., *Mol. Biol. Cell* 2003, *14*, 4654–4666.

[51] Wylie, S. R., Wu, P.-J., Patel, H., Chantler, P. D., *Proc. Natl. Acad. Sci. USA* 1998, *95*, 12967–12972.

[52] Diefenbach, T. J., Latham, V. M., Yimlamai, D., Liu, C. A. *et al.*, *J. Cell Biol.* 2002, *158*, 1207–1217.

[53] Ma, X., Kawamoto, S., Hara, Y., Adelstein, R. S., *Mol. Biol. Cell* 2004, *15*, 2568–2579.

[54] Iwami, Y., Ojima, T., Inoue, A., Nishita, K., *Comp. Biochem. Physiol. B* 2002, *133*, 257–267.

[55] Yaffe, M. B., Farr, G. W., Miklos, D., Horwich, A. L. *et al.*, *Nature* 1992, *358*, 245–248.

[56] Gao, Y., Thomas, J. O., Chow, R. L., Lee, G.-H., Cowan, N. J., *Cell* 1992, *69*, 1043–1050.

[57] Roobol, A., Holmes, F. E., Hayes, N. V. L., Baines, A. J., Carden, M. J., *J. Cell Sci.* 1995, *108*, 1477–1488.

[58] Littlefield, R., Almenar-Queralt, A., Fowler, V. M., *Nat. Cell Biol.* 2001, *3*, 544–551.

[59] Weber, A., Pennise, C. R., Babcock, G. G., Fowler, V. M., *J. Cell Biol.* 1994, *127*, 1627–1635.

[60] Fischer, R. S., Fowler, V. M., *Trends Cell Biol.* 2003, *13*, 593–601.

[61] Fischer, R. S., Fritz-Six, K. L., Fowler, V. M., *J. Cell Biol.* 2003, *161*, 371–380.

[62] Leung, C. L., Zheng, M., Prater, S. M., Liem, R. K. H., *J. Cell Biol.* 2001, *154*, 691–697.

[63] Yang, Y., Dowling, J., Yu, Q.-C., Kouklis, P. *et al.*, *Cell* 1996, *86*, 655–665.

[64] Becker, J., Craig, E. A., *Eur. J. Biochem.* 1994, *219*, 11–23.

[65] Gething, M.-J., Sambrook, J., *Nature* 1992, *355*, 33–45.

[66] Haas, I. G., *Experientia* 1994, *50*, 1012–1020.

[67] Kiang, J. G., Tsokos, G. C., *Pharmacol. Ther.* 1998, *80*, 183–201.

[68] Wang, S., Longo, F. M., Chen, J., Butman, M. *et al.*, *Neurochem. Int.* 1993, *23*, 575–582.

[69] Little, E., Tocco, G., Baudry, M., Lee, A. S., Schreiber, S. S., *Neuroscience* 1996, *75*, 209–219.

[70] Terao, A., Steininger, T. L., Hyder, K., Apte-Deshpande, A. *et al.*, *Neuroscience* 2003, *116*, 187–200.

[71] Tsuchiya, D., Hong, S., Matsumori, Y., Kayama, T. *et al.*, *Neurosurgery* 2003, *53*, 1179–1187.

[72] Grosche, J., Härtig, W., Reichenbach, A., *Neurosci. Lett.* 1995, *185*, 119–122.

[73] Härtig, W., Grosche, J., Distler, C., Grimm, D. *et al.*, *J. Neurocytol.* 1995, *24*, 507–517.

[74] Lewis, G. P., Erickson, P. A., Guérin, C. J., Anderson, D. H., Fisher, S. K., *Exp. Eye Res.* 1989, *49*, 93–111.

[75] Lewis, G. P., Guérin, C. J., Anderson, D. H., Matsumoto, B., Fisher, S. K., *Am. J. Ophthalmol.* 1994, *118*, 368–376.

[76] Oliver, C. N., Starke-Reed, P. E., Stadtman, E. R., Liu, G. J. *et al.*, *Proc. Natl. Acad. Sci. USA* 1990, *87*, 5144–5147.

[77] Smith, C. D., Carney, J. M., Starke-Reed, P. E., Oliver, C. N. *et al.*, *Proc. Natl. Acad. Sci. USA* 1991, *88*, 10540–10543.

[78] Gorovits, R., Avidan, N., Avisar, N., Shaked, I., Vardimon, L., *Proc. Natl. Acad. Sci. USA* 1997, *94*, 7024–7029.

[79] Lai, J. C. K., Murthy, C. R. K., Cooper, A. J. L., Hertz, E., Hertz, L., *Neurochem. Res.* 1989, *14*, 377–389.

[80] Bajo, M., Fruehauf, J., Kim, S. H., Fountoulakis, M., Lubec, G., *Proteomics* 2002, *2*, 1539–1546.

[81] Sensenbrenner, M., Lucas, M., Deloulme, J.-C., *J. Mol. Med.* 1997, *75*, 653–663.

[82] Giallongo, A., Oliva, D., Cali, L., Barba, G. *et al.*, *Eur. J. Biochem.* 1990, *190*, 567–573.

[83] Slemmer, J. E., Weber, J. T., De Zeeuw, C. I., *Neurobiol. Dis.* 2004, *15*, 563–572.

[84] Lin, R. C. S., Matesic, D. F., *Neuroscience* 1994, *60*, 11–16.

[85] Hattori, T., Takei, N., Mizuno, Y., Kato, K., Kohsaka, S., *Neurosci. Res.* 1995, *21*, 191–198.

[86] Li, A., Lane, W. S., Johnson, L. V., Chader, G. J., Tombran-Tink, J., *J. Neurosci.* 1995, *15*, 385–393.

[87] Takei, N., Kondo, J., Nagaike, K., Ohsawa, K. *et al.*, *J. Neurochem.* 1991, *57*, 1178–1184.

[88] Yoshida, M., Muneyuki, E., Hisabori, T., *Nat. Rev. Mol. Cell Biol.* 2001, *2*, 669–677.

[89] Sofroniew, M. V., Howe, C. L., Mobley, W. C., *Annu. Rev. Neurosci.* 2001, *24*, 1217–1281.

[90] Kendall, G., Ensor, E., Crankson, H. D., Latchman, D. S., *Eur. J. Biochem.* 1996, *236*, 360–364.

[91] Wieczorek, H., Brown, D., Grinstein, S., Ehrenfeld, J., Harvey, W. R., *Bioessays* 1999, *21*, 637–648.

[92] Gogarten, J. P., Starke, T., Kibak, H., Fishmann, J., Taiz, L., *J. Exp. Biol.* 1992, *172*, 137–147.

[93] Manabe, T., Yoshimori, T., Henomatsu, N., Tashiro, Y., *J. Cell Physiol.* 1993, *157*, 445–452.

[94] Melin, P., Schnürer, J., Wagner, E. G. H., *Microbiology* 2004, *150*, 743–748.

[95] Otani, H., Yamamura, T., Nakao, Y., Hattori, R. *et al.*, *Circulation* 2000, *102*, III269–III274.

[96] Zhan, H., Yokoyama, K., Otani, H., Tanigaki, K. *et al.*, *Genes Cells* 2003, *8*, 501–513.

[97] Wang, H.-G., Pathan, N., Ethell, I. M., Krajewski, S. *et al.*, *Science* 1999, *284*, 339–343.

[98] Shibasaki, F., Hallin, U., Uchino, H., *J. Biochem. (Tokyo)* 2002, *131*, 1–15.

[99] Nottingham, S., Knapp, P., Springer, J., *Exp. Neurol.* 2002, *177*, 242–251.

[100] Sharkey, J., Butcher, S. P., *Nature* 1994, *371*, 336–339.

[101] Terada, H., Matsushita, M., Lu, Y.-F., Shirai, T. *et al.*, *J. Neurochem.* 2003, *87*, 1145–1151.

[102] Bukau, B., Horwich, A. L., *Cell* 1998, *92*, 351–366.

[103] Hartl, F. U., *Nature* 1996, *381*, 571–579.

[104] Santacruz, H., Vriz, S., Angelier, N., *Dev. Genet.* 1997, *21*, 223–233.

[105] Vega-Núñez, E., Peña-Melián, A., de la Rosa, E. J., de Pablo, F., *Mech. Dev.* 1999, *82*, 199–203.

[106] Popanda, O., Fox, G., Thielmann, H. W., *Biochim. Biophys. Acta* 1998, *1397*, 102–117.

[107] Vishwanatha, J. K., Jindal, H. K., Davis, R. G., *J. Cell Sci.* 1992, *101*, 25–34.

[108] Hans, P., Born, J. D., Chapelle, J.-P., Milbouw, G., *J. Neurosurg.* 1983, *58*, 689–692.

[109] Kaste, M., Hernesniemi, J., Somer, H., Hillbom, M., Konttinen, A., *J. Neurosurg.* 1981, *55*, 511–515.

[110] Kaste, M., Somer, H., Konttinen, A., *Arch. Neurol.* 1977, *34*, 142–144.

[111] Schlattner, U., Möckli, N., Speer, O., Werner, S., Wallimann, T., *J. Invest. Dermatol.* 2002, *118*, 416–423.

[112] Askenasy, N., Koretsky, A. P., *Am. J. Physiol.* 1997, *273*, C741–C746.

[113] Han, Z.-G., Zhang, Q.-H., Ye, M., Kan, L.-X. *et al.*, *J. Biol. Chem.* 1999, *274*, 35741–35748.

[114] Lee, T. H., Lwu, S., Kim, J., Pelletier, J., *J. Biol. Chem.* 2002, *277*, 44826–44837.

